Title

Type II Diabetes Mellitus Causes Extracellular Matrix Alterations in the Posterior Cornea That Increase Graft Thickness and Rigidity.

Journal

Investigative ophthalmology & visual science, 64(7)

ISSN

0146-0404

Authors

Kingsbury, Kenten D
Skeie, Jessica M
Cosert, Krista
et al.

Publication Date

2023-06-01

DOI

10.1167/iovs.64.7.26

Peer reviewed

Type II Diabetes Mellitus Causes Extracellular Matrix Alterations in the Posterior Cornea That Increase Graft Thickness and Rigidity

Kenten D. Kingsbury,[1,2] Jessica M. Skeie,[1,2] Krista Cosert,[3,4] Gregory A. Schmidt,[2] Benjamin T. Aldrich,[1,2] Christopher S. Sales,[1,2] Julia Weller,[5] Friedrich Kruse,[5] Sara M. Thomasy,[3,4] Ursula Schlötzer-Schrehardt,[5] and Mark A. Greiner[1,2]

[1]Department of Ophthalmology and Visual Sciences, Carver College of Medicine, University of Iowa, Iowa City, Iowa, United States
[2]Iowa Lions Eye Bank, Coralville, Iowa, United States
[3]Department of Surgical & Radiological Sciences, School of Veterinary Medicine, University of California, Davis, Davis, California, United States
[4]Department of Ophthalmology & Vision Science, School of Medicine, University of California, Davis, Davis, California, United States
[5]Department of Ophthalmology, Friedrich-Alexander-University Erlangen-Nürnberg, Erlangen, Germany

Correspondence: Mark A. Greiner, Department of Ophthalmology and Visual Sciences, Carver College of Medicine, University of Iowa, 200 Hawkins Drive, Iowa City, IA 52242, USA;
mark-greiner@uiowa.edu.
Ursula Schlötzer-Schrehardt, Department of Ophthalmology, Friedrich-Alexander-University Erlangen-Nürnberg, Schwabachanlage 6, 91054 Erlangen, Germany;
ursula.schloetzer-schrehardt@uk-erlangen.de.

USS and MAG contributed equally to the work presented here and should therefore be regarded as equivalent authors.

Received: March 15, 2023
Accepted: May 11, 2023
Published: June 16, 2023

Citation: Kingsbury KD, Skeie JM, Cosert K, et al. Type II diabetes mellitus causes extracellular matrix alterations in the posterior cornea that increase graft thickness and rigidity. *Invest Ophthalmol Vis Sci.* 2023;64(7):26.
https://doi.org/10.1167/iovs.64.7.26

Purpose. There is a pressing need to investigate the impact of type II diabetes mellitus on the posterior cornea in donor tissues given its increasing prevalence and potential impact on endothelial keratoplasty surgical outcomes.

Methods. Immortalized human cultured corneal endothelial cells (CECs; HCEC-B4G12) were grown in hyperglycemic media for 2 weeks. Extracellular matrix (ECM) adhesive glycoprotein expression and advanced glycation end products (AGEs) in cultured cells and corneoscleral donor tissues, as well as the elastic modulus for the Descemet membrane (DMs) and CECs of diabetic and nondiabetic donor corneas, were measured.

Results. In CEC cultures, increasing hyperglycemia resulted in increased transforming growth factor beta-induced (TGFBI) protein expression and colocalization with AGEs in the ECM. In donor corneas, the thicknesses of the DM and the interfacial matrix (IFM) between the DM and stroma both increased from 8.42 ± 1.35 µm and 0.504 ± 0.13 µm in normal corneas, respectively, to 11.13 ± 2.91 µm (DM) and 0.681 ± 0.24 µm (IFM) in non-advanced diabetes ($P = 0.013$ and $P = 0.075$, respectively) and 11.31 ± 1.76 µm (DM) and 0.744 ± 0.18 µm (IFM) in advanced diabetes (AD; $P = 0.0002$ and $P = 0.003$, respectively). Immunofluorescence in AD tissues versus controls showed increased AGEs ($P < 0.001$) and markedly increased labeling intensity for adhesive glycoproteins, including TGFBI, that colocalized with AGEs. The elastic modulus significantly increased between AD and control tissues for the DMs ($P < 0.0001$) and CECs ($P < 0.0001$).

Conclusions. Diabetes and hyperglycemia alter human CEC ECM structure and composition, likely contributing to previously documented complications of endothelial keratoplasty using diabetic donor tissue, including tearing during graft preparation and reduced graft survival. AGE accumulation in the DM and IFM may be a useful biomarker for determining diabetic impact on posterior corneal tissue.

Keywords: corneal endothelial cells, corneal biomechanics, corneal transplantation

According to the National Diabetes Statistics Report published by the Centers for Disease Control and Prevention, 37.3 million people in the United States (11.3%) have diabetes mellitus.[1] Corneal transplantation already is widely affected by the high prevalence of diabetes due to the inclusion of corneal tissues from donors with a known diagnosis of diabetes mellitus in the transplant pool (37% in 2017).[2] Diabetic donor corneal tissue was associated with greater endothelial cell loss and higher rates of graft failure 3 years postoperatively after Descemet stripping automated endothelial keratoplasty.[3] We previously reported that morphological, biochemical, and functional changes can be observed in the corneal endothelium–Descemet membrane tissue complex (EDM) from cornea donors with diabetes.[2–5] Liaboe and colleagues[2] documented that corneal tissue from donors with medical complications resulting from insulin-dependent diabetes have increased cell loss and lower endothelial cell density compared to age-matched

Investigative Ophthalmology & Visual Science

controls. In addition to impairment in cell function, there are structural impairments that affect the posterior cornea and the EDM as a functional tissue unit.[6] Diabetic donor corneal tissues have a higher failure rate of graft preparation for Descemet membrane endothelial keratoplasty (DMEK), approximately 9.2 times greater than that of nondiabetic controls,[7] and it occurs more frequently with longer disease duration.[7,8] Increased structural adhesion between the Descemet membrane (DM) and the posterior stroma has also been demonstrated in corneal tissues from insulin-dependent donors with end-organ damage (e.g., retinopathy, nephropathy, neuropathy) using a high-fidelity model of DMEK graft preparation.[9] In aggregate, these studies suggest that diabetes mellitus imparts changes to the posterior cornea that impact clinical care.[2]

In this investigation, we studied the impact of diabetes on the extracellular matrix (ECM) of the corneal endothelium, with particular focus on the interfacial matrix (IFM) between the DM and posterior stroma that forms a cleavage plane of high clinical relevance to DMEK graft preparation and resection of diseased tissue.[10] We hypothesized that diabetic hyperglycemia results in structural alterations to ECM proteins in the IFM, particularly the formation of advanced glycation end products (AGEs) that result from nonenzymatic glycation and oxidation; participate in reactive oxygen species formation; and form cross-links. Using a controlled hyperglycemia cell culture model, we evaluated how CECs respond to increasing hyperglycemic conditions to establish a dose–response. We characterized key IFM protein expression changes, glycation events, and ECM alterations occurring in diabetic donor corneal tissue which varied by severity of disease versus age-matched controls, and we utilized transmission electron microscopy and immunohistochemistry to visualize IFM protein expression changes and structural alterations. Additionally, atomic force microscopy was used to quantify the integrity and resistance to deformational forces of DMEK prepared diabetic and control tissues to investigate the biomechanical impact of diabetes. Understanding the impact of diabetes mellitus on cellular and extracellular structures in the posterior cornea may provide biochemical markers for grading tissue health and a basis for improved therapeutic options for patients that require corneal transplantation.

Methods

Cell Culture

Immortalized human corneal endothelial cells (HCEC-B4G12; DSMZ, Braunschweig, Germany) were cultured as previously described.[11] To create a cell culture model that reproduced the hyperglycemic conditions to which diabetic corneal endothelial cells are exposed in the anterior chamber,[12] HCEC-B4G12 cells were cultured in four separate D-glucose–supplemented culture media conditions. The control group was grown in a 5.5-mM (99.10 mg/dL) glucose medium to simulate a normoglycemic, physiological environment. The other conditions used hyperglycemic solutions of 13.0 mM (234.23 mg/dL), 30.5 mM (549.55 mg/dL), and 105.5 mM (1900.90 mg/dL) glucose, recapitulating increasing hyperglycemic concentration. These four glucose conditions correspond to hemoglobin A1c values of 5.1%, 9.8%, 20.8%, and 68%, respectively. Confluent cell cultures were grown in each glucose condition for 2 weeks prior to use in experiments.

Table 1. Donor Demographic Information

No.	Diagnosis	Age (y)	Sex	No.	Diagnosis	Age (y)	Sex
1	AD	46	M	26	ND	70	F
2	AD	65	F	27	ND	70	F
3	AD	71	M	28	ND	61	M
4	AD	60	M	29	ND	49	F
5	NAD	69	M	30	ND	73	F
6	NAD	74	M	31	NAD	74	M
7	NAD	57	M	32	NAD	70	M
8	NAD	71	F	33	NAD	59	M
9	NAD	70	F	34	NAD	66	M
10	ND	65	F	35	NAD	68	F
11	ND	72	M	36	AD	64	M
12	ND	57	M	37	AD	72	F
13	ND	48	F	38	AD	55	F
14	ND	21	M	39	AD	55	M
15	ND	58	M	40	AD	66	F
16	ND	51	M	41	AD	56	M
17	ND	73	F	42	AD	58	F
18	ND	56	M	43	AD	69	F
19	ND	56	F	44	AD	62	F
20	ND	70	F	45	AD	72	F
21	ND	56	F	46	DM, unspecified	61	M
22	ND	59	F	47	DM, unspecified	64	M
23	ND	71	F	48	DM, unspecified	66	M
24	ND	63	F	49	DM, unspecified	61	F
25	ND	78	F	50	DM, unspecified	55	M

Demographic and medical history information for donors with or without type II diabetes mellitus analyzed for proteomic changes via western blotting (1–14), transmission electron microscopy (15–50), and immunohistochemistry (15–50). See Supplementary Table S1 for additional donor information. DM, diabetes mellitus.

Donor Tissues

This study was determined to be exempt by the University of Iowa's Institutional Review Board and adheres to the tenets of the Declaration of Helsinki. None of the donor tissues procured and used for this investigation was from a vulnerable population, and all donors or next of kin provided appropriate consent for tissue donation and research. Corneoscleral tissue was obtained from 50 cornea donors 21 to 75 years of age and stored in Optisol-GS (Bausch & Lomb, Rochester, NY, USA) at 4°C. EDM tissue samples were assigned to one of three groups: no diabetes (ND), non-advanced diabetes (NAD), and advanced diabetes (AD). The ND group included donors with no known history of diabetes. The NAD group included donors with a history of diabetes but without a history of end-organ damage secondary to diabetes. The AD group included donors with a history of diabetes that had a history of end-organ damage secondary to diabetes.[2,4,9] All disease group donors had type 2 diabetes mellitus and no known corneal diseases. Donor demographics are summarized in Table 1.

Transmission Electron Microscopy

For transmission electron microscopy, donor corneal tissues were fixed, embedded, sectioned, and examined with a transmission electron microscope (EM906E; Carl Zeiss Microscopy, Oberkochen, Germany) as previously described.[13] Briefly, we used 2.5% glutaraldehyde in 0.1-M phosphate buffer to fix the donor corneas samples, and then they were postfixed in 2% buffered osmium tetroxide. Corneas were serially dehydrated and then embedded

Table 2. Primary Antibodies Used for Immunohistochemistry

Antibody (Clone), Host Species	Antibody Concentration	Application	Antibody Source
AGEs, rabbit polyclonal	1:4000	Immunohistochemistry	Abcam
AGEs (6D12)	1:100	Immunohistochemistry	TransGenic
Amyloid P, rabbit polyclonal	1:300	Immunohistochemistry	Dako Diagnostics
CML (NF-1G)	1:200	Immunohistochemistry	Abcam
Collagen type III (1E7-D7)	1:200	Immunohistochemistry	Merck Millipore
Collagen type IV (2F11)	1:50	Immunohistochemistry	Southern Biotech
Fibronectin (IST-4)	1:50	Immunohistochemistry	Sigma-Aldrich
Tenascin-C, rabbit polyclonal	1:200	Immunohistochemistry	Merck Millipore
TGFBI, rabbit polyclonal	1:2000	Immunohistochemistry	Sigma-Aldrich
Vitronectin (VN58-1)	1:50	Immunohistochemistry	Abcam

in epoxy resin using a standard procedure. Prior to examination with the EM906E transmission electron microscope, ultrathin sections (80 nm) were stained with uranyl acetate and lead citrate.

Immunohistochemistry

Immunohistochemistry was performed using a panel of antibodies against adhesive matrix glycoproteins (fibronectin, vitronectin, amyloid P, tenascin-C, transforming growth factor beta-induced [TGFBI]) and AGEs, including carboxymethyl-lysine (CML), as previously described.[13] Briefly, cryostat-cut corneal sections (5 µm) were blocked with 10% normal goat serum prior to primary antibodies diluted in phosphate-buffered saline (PBS) being added and incubated overnight at 4°C. Alexa Fluor 488- and Alexa Fluor 555-conjugated secondary antibodies (Molecular Probes, Eugene, OR, USA) were used to detect antibody binding. 4′,6-Diamidino-2-phenylindole (DAPI; Sigma-Aldrich, St. Louis, MO, USA) was used as a nuclear counterstain. Using 20× magnification, three images per specimen were used to quantitatively analyze the fluorescence intensity values of AGE staining. ImageJ software (National Institutes of Health, Bethesda, MD, USA) was used to correct for negative control background.

Immunogold labeling was performed as previously described.[14] Briefly, 4% paraformaldehyde and 0.1% glutaraldehyde in 0.1-M cacodylate buffer (pH 7.4) were used to fix corneal tissue samples prior to dehydration and being embedded in resin (LR White; Electron Microscopy Sciences, Hatfield, PA, USA). Ultrathin sections were successively incubated with Tris-buffered saline (TBS), 0.05-M glycine in TBS, 0.5% ovalbumin and 0.5% fish gelatin in TBS, and primary antibodies diluted in TBS–ovalbumin overnight at 4°C. Next, samples were incubated with 10 nm gold-conjugated secondary antibodies (Aurion Biotech, Seattle, WA, USA). When incubation was complete, uranyl acetate was used to stain the sections. The sections were observed with a transmission electron microscope. Primary antibodies used are summarized in Table 2.

Separately, cultured HCEC-B4G12 samples grown in the various hyperglycemic culture conditions were labeled with antibodies against the adhesive matrix glycoproteins fibronectin (MilliporeSigma, Burlington, MA, USA), vitronectin (MilliporeSigma), and TGFBI (Thermo Fisher Scientific, Waltham, MA, USA), and AGEs (Abcam, Cambridge, UK). Cells were chemically removed from the underlying adhesive ECM, digested with 150 µL of radioimmunoprecipitation assay (RIPA) buffer at room temperature for 1.5 minutes, and removed. The extracellular matrix still adhered to the coverslips was fixed with a 4% paraformaldehyde solution (PFA, pH 7.4) for 10 minutes. For immunofluorescent staining, matrices were blocked with 100 µL of 1% bovine or horse serum diluted in PBS for 15 minutes and rinsed once with 200 µL of PBS. The primary antibody was then added to the coverslips at 5 µg/mL diluted in PBS with a total volume of 100 µL per coverslip and incubated at room temperature for 2 hours. For TGFBI, a polyclonal rabbit immunoglobulin G (IgG) anti-TGFBI primary antibody (Thermo Fisher Scientific) was used, and a polyclonal goat IgG anti-AGE primary antibody (Abcam) was used to target AGEs. Anti-vitronectin (MilliporeSigma) and anti-fibronectin (MilliporeSigma) IgG anti-bodies were also used for respective analyses. Following three rinses with PBS, 100 µL per coverslip of species-specific secondary antibody (Alexa Fluor 488 [antiAGE] or Alexa Fluor 546 [anti-TGFBI, vitronectin, fibronectin]; Thermo Fisher Scientific) at 1:1000 dilution in PBS with DAPI was added and incubated for 60 minutes at room temperature. After an additional three rinses with PBS solution, the coverslips were mounted onto a slide using ProLong Diamond Antifade Mountant (Thermo Fisher Scientific) for immunofluorescent microscopy visualization. Matrices were imaged using confocal microscopy.

Automated Microfluidic Western Blotting

Hyperglycemic HCEC-B4G12 CECs were lysed for both cytosolic cell and ECM fractions of proteins. CEC fractions were collected by digesting with RIPA buffer detergent for 3 minutes, and the ECM was digested with a collagenase/hyaluronidase (Worthington Biochemical, Lakewood, NJ, USA) mixture for 6 hours. Protein detection was performed using automated microfluidic western blotting on a ProteinSimple Jess machine (bio-techne, Minneapolis, MN, USA) and analyzed using ProteinSimple Compass software. A polyclonal goat IgG anti-AGE primary antibody (Abcam) was used to detect AGEs. The abundance of proteins was normalized to total protein in each sample and compared among the different groups of cells or matrices.

Atomic Force Microscopy

Corneal samples were prepared for measurement with atomic force microscopy (AFM) as previously described.[15] Briefly, a standard Petri dish was coated with a layer of silicone (SYLGARD 527 Silicone Dielectric Gel, 24-hour cure at room temperature; Dow, Midland, MI, USA) and a 2-mm biopsy punch was used to create a window in a 13-mm Thermanox coverslip (Thermo Fisher Scientific). Corneas were cut into quarters. One quarter was incubated in 2.5-mM

Investigative Ophthalmology & Visual Science

EDTA in HEPES buffer for 30 minutes and sonicated for 5 minutes to remove endothelial cells and expose the DM, and a different quarter with intact endothelium was mounted. Due to the thickness of human corneas, a portion of the silicone substrate was cut to match the shape of the tissue piece to be mounted and removed, and the cornea samples were gently fit into the resulting depression with the endothelium or DM facing up. The outer edge of the coverslip was dotted with cyanoacrylate glue and applied such that the window would grant access to the endothelium or exposed DM without glue coming into contact with the tissue. The sample was then fully submerged in Dulbecco's phosphate-buffered saline (DPBS) to cure the glue and maintain tissue hydration during measurements. All force measurements were done using a MFP-3D-BIO atomic force microscope (Asylum Research, Oxford Instruments, Santa Barbara, CA, USA) and PNP-TR-50 silicon nitride cantilevers with nominal spring constants of 0.32 N/m and 35° half-angle openings modified with a 5-µm-diameter borosilicate bead (Thermo Fisher Scientific). Immediately prior to use, cantilevers were calibrated for the deflection inverse optical lever sensitivity (Defl InvOLS) by indentation in DPBS on glass and then calibrated for the spring constant by the thermal method in DPBS using the Asylum Research software. The maximum indentation force was set at 5 nN. Each cornea was probed at 10 unique locations with five force curves collected per location at a scan velocity of 1.98 µm/s. The point of probe contact with the cornea was determined by a masked analyst, and the elastic modulus was determined by fitting the force curves to the Hertz model for spherical geometry as described previously.[16]

Statistical Analysis

For the immunohistochemistry of embedded donor corneal tissues, statistical significance was determined using a two-tailed *t*-test or the nonparametric Mann–Whitney *U* test. The resulting elastic moduli data for automated force microscopy were determined to be non-normal via the Shapiro–Wilk test, and subsequently significance was determined via a Mann–Whitney–Wilcoxon rank-sum test.

Results

Increasing Hyperglycemia Results in Increased Deposition and Colocalization of TGFBI and AGEs in the ECM of Immortalized CECs

Cultured CECs were assayed using immunohistochemistry and microfluidics western blotting to assess ECM protein alterations in the posterior cornea associated with diabetic hyperglycemia. Increasing hyperglycemia resulted in increased TGFBI and AGE deposition in the ECM of

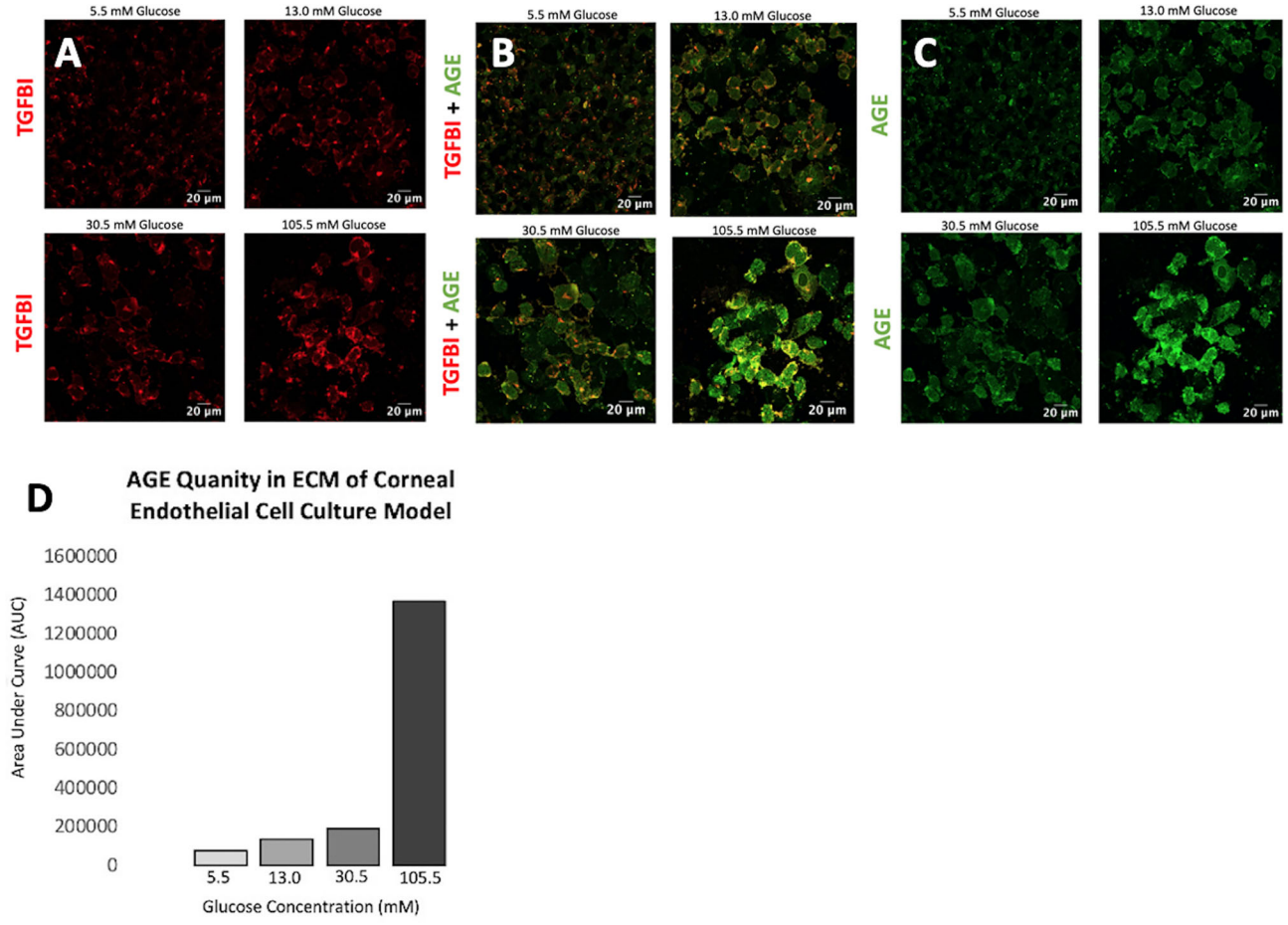

Figure 1. Increased deposition of TGFBI and AGEs in the ECM of immortalized corneal endothelial cells with colocalization of TGFBI and glycation events. Immunohistochemistry images showing (**A**) TGFBI, (**C**) AGE expression, and (**B**) colocalized expression in the ECM of immortalized cultured corneal endothelial cells. (**D**) Increased AGE quantification in the ECM of immortalized cultured corneal endothelial cells based on western blotting data.

Investigative Ophthalmology & Visual Science

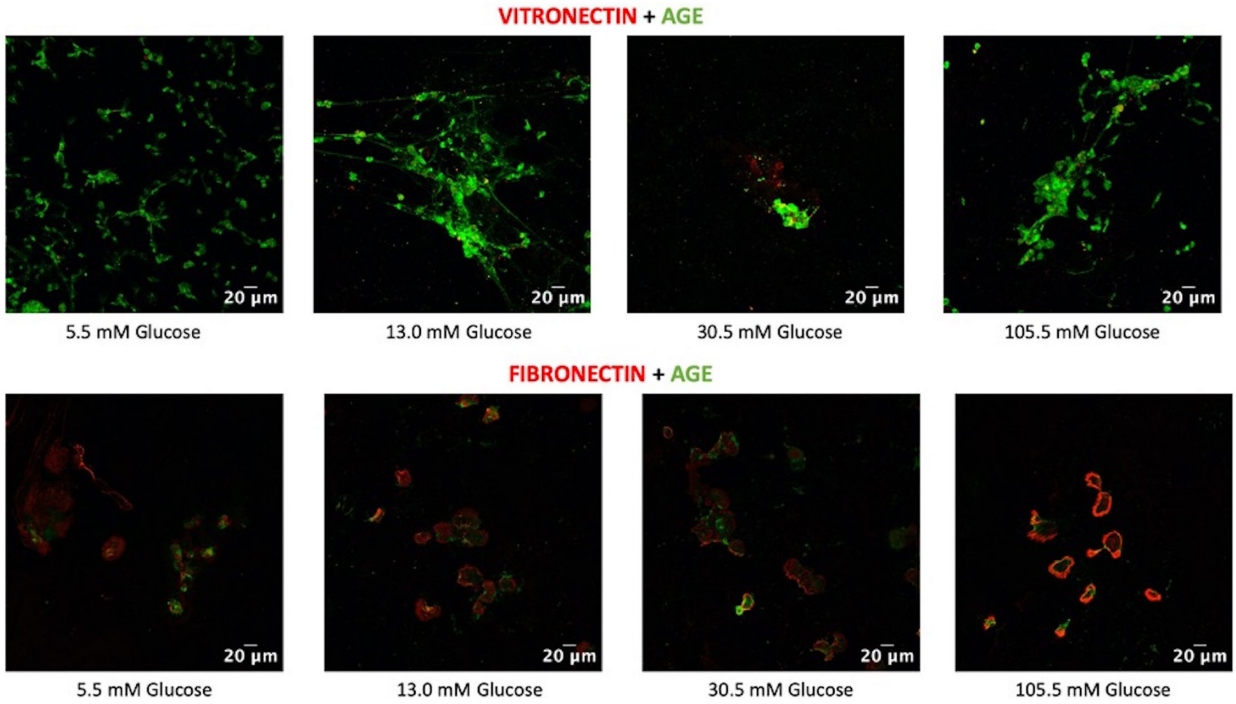

Figure 2. Vitronectin and fibronectin do not colocalize with AGEs in immortalized cultured corneal endothelial cells under varying concentrations of glucose. (*Top*) Immunohistochemistry showing consistent vitronectin fluorescent signal with increasing hyperglycemic concentration and lack of colocalization with AGEs at all glucose concentrations in merged signals. (*Bottom*) Immunohistochemistry showing increased fibronectin fluorescent signal in the 105.5-mM glucose concentration and lack of colocalization with AGEs at all glucose concentrations in merged signals.

immortalized CECs. Merged fluorescent images showed the colocalization of TGFBI and glycation events (Fig. 1). Quantification of AGEs via western blot analysis showed an increasing amount of glycated end products with rising hyperglycemic concentration (Fig. 1). Increased fibronectin fluorescent signal appeared in the 105.5-mM glucose environment and remained at a relatively stable intensity throughout the other glycemic concentrations. Merging of the fluorescent signals of fibronectin and AGE showed a lack of colocalization. The immunohistochemistry of vitronectin showed no significant increase in fluorescent signal with the rising hyperglycemic concentrations. In addition, when the vitronectin and AGE fluorescent signals were merged, the signal did not appear to colocalize (Fig. 2).

Diabetic Donor Corneas Exhibit Ultrastructural Alterations and Increased Thickness of DM and the DM–Stroma IFM

Transmission electron microscopy and immunohistochemistry were performed in order to visualize the structural alterations in the DMs and CECs of diabetic and control donor corneal tissues. EDM tissue samples were assigned to one of three groups according to the diabetes status of the donor and severity of disease determined through medical records review: ND, NAD, or AD.[2,4,9] In total, 20 diabetic (10 NAD, 10 AD) and 10 nondiabetic control donor corneas were analyzed by transmission electron microscopy to assess ultrastructural changes in the posterior cornea associated with diabetes. Donor demographics are summarized in Table 1. Compared to normal control corneas, diabetic corneas demonstrated irregular CECs containing intra- and intercellular vacuoles, abundant mitochondria, prominent Golgi bodies, and lysosomal inclusions (Fig. 3). CECs in diabetic corneas also showed blebbing, a compacted apical membrane, and an irregular apical surface. DM thickness was significantly increased, from 8.42 ± 1.35 µm in normal corneas to 11.13 ± 2.91 µm in NAD ($P = 0.013$) and 11.31 ± 1.76 µm ($P = 0.0002$) in AD corneas (Fig. 3). In diabetic corneas, abnormal vacuolar inclusions could be frequently observed at the DM–stroma interface along with abnormal collagen inclusions within the posterior portions of DM close to the endothelial layer (eight of 20 corneas). These inclusions consisted of long-spacing collagen bundles, which were positive for collagen type III by immunofluorescence labeling. By contrast, control corneas exhibited a homogeneous posterior nonbanded layer of DM devoid of any vacuolar or fibrillar inclusions (Fig. 3). Additionally, transmission electron microscopy was used to show the structural alterations of the DM–stroma interface in diabetic and normal control corneas. Diabetic corneas showed an increase in thickness of the IFM compared to control corneas. This DM–stroma boundary in diabetic corneas also showed variable amounts of vacuolar inclusions that were not observed in control tissues (Fig. 4). Smaller vacuoles could be seen to coalesce to spacious accumulations in some specimens. The mean thickness of the IFM was 0.681 ± 0.24 µm in NAD and 0.744 ± 0.18 µm in AD corneas compared to 0.504 ± 0.13 µm in control corneas ($P = 0.075$ and $P = 0.003$, respectively).

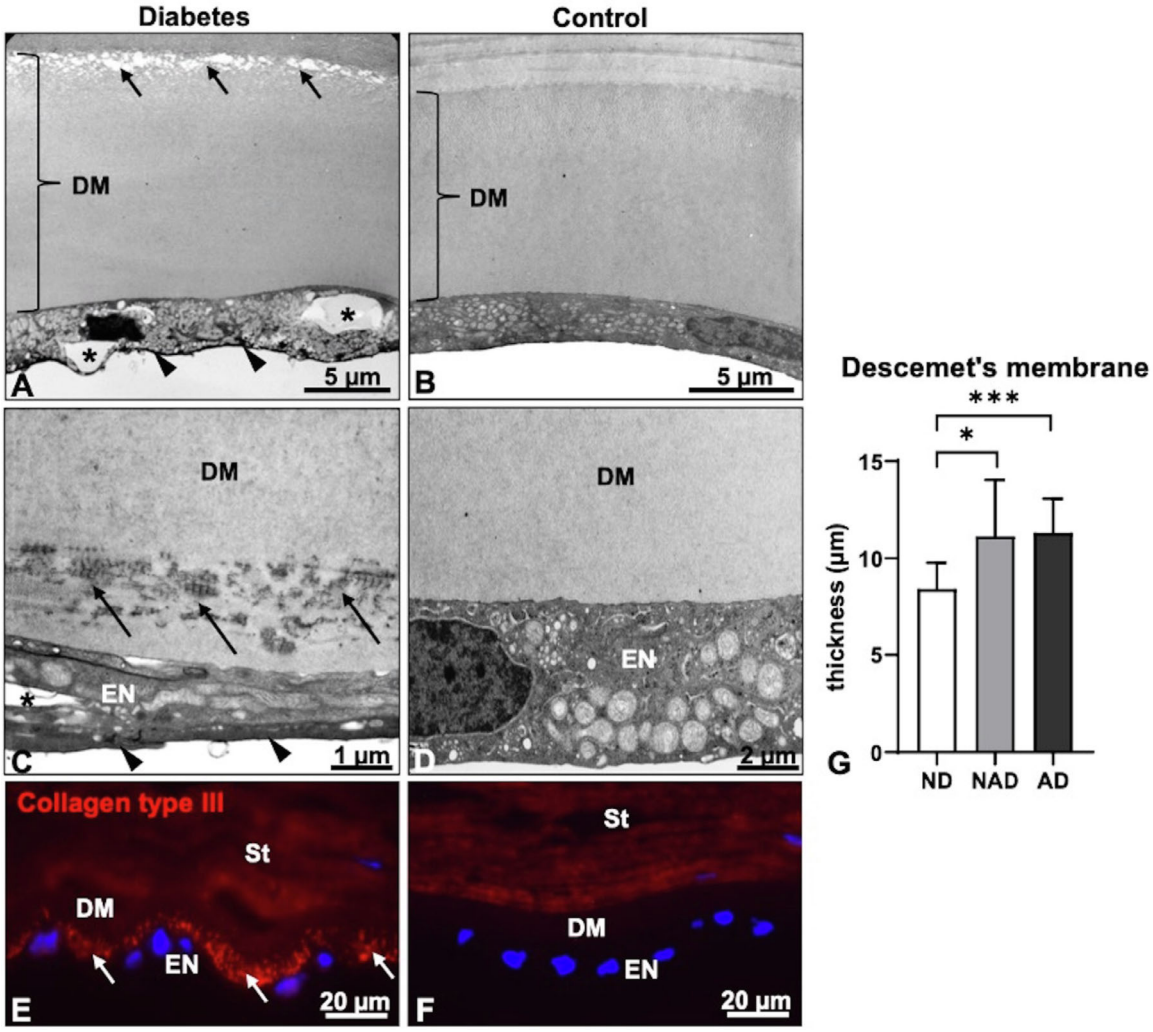

Figure 3. Structural alterations of the DM and endothelium in diabetic and normal control corneas. (**A**–**D**) Transmission electron micrographs showing thickened DM with accumulations of vacuolar inclusions at the DM–stroma interface (**A**, *arrows*) and long-spacing collagen inclusions close to the endothelial layer (EN) (**C**, arrows) in association with diabetes. The diabetic endothelium shows irregularities such as vacuoles, blebs (**A**, **C**, *asterisks*), and a compacted apical surface (**A**, **C**, *arrowheads*). (**E**, **F**) Immunohistochemical analysis showing differential staining patterns of the DM for collagen type III in diabetic (**E**, *arrows*) compared to normal corneas. Nuclei are counterstained with DAPI (*blue*); St, stroma. (**G**) Quantitative analysis of DM thickness in ND, NAD, and AD corneas. Data are expressed as means ± SD ($n = 10$ in each group); $^{*}P = 0.013$, $^{***}P = 0.0002$ (*t*-test).

AGEs Form on Adhesive Matrix Glycoproteins at the IFM of Diabetic Donor Corneas

Immunohistochemistry was used to further characterize the DM–stroma interface in diabetic donor corneas with attention to detecting and quantifying accumulations of AGEs and adhesive glycoproteins predicted at that location. In all diabetic corneas (10 NAD, 10 AD), increased AGE immunoreactivity was observed in the epithelial basement membrane (not shown) and in the corneal stroma, particularly in the posterior stroma and along the DM–stroma interface region (Fig. 5). Similar staining patterns were obtained with polyclonal and monoclonal antibodies against AGEs, as well with antibodies against CML, a major AGE species found in tissues.[17] Quantitative analysis of immunofluorescence signals using ImageJ confirmed increased amounts of AGEs in diabetic versus nondiabetic corneas ($P < 0.001$). AGE immunoreactivity was also increased over the negative background control in nondiabetic control corneas ($P = 0.004$) (Fig. 5). Adhesive glycoproteins, including vitronectin, fibronectin, amyloid P, TGFBI, and tenascin-C, as well as collagen type IV, were present along the DM–stroma interface in both diabetic and control corneas. However, labeling intensity was markedly increased in diabetic specimens (Fig. 6). Additionally, immunohistochemistry and transmission electron microscopy double-labeling experiments detected colocalization of adhesive glycoproteins with AGEs at the DM–stroma interface in diabetic and normal control corneas (Fig. 7).

Diabetic Donor DMEK Tissues Have Stiffer DM and Endothelial Cells

As changes in ECM stiffness have been shown to have a pathological impact on CEC health in other diseases

Investigative Ophthalmology & Visual Science

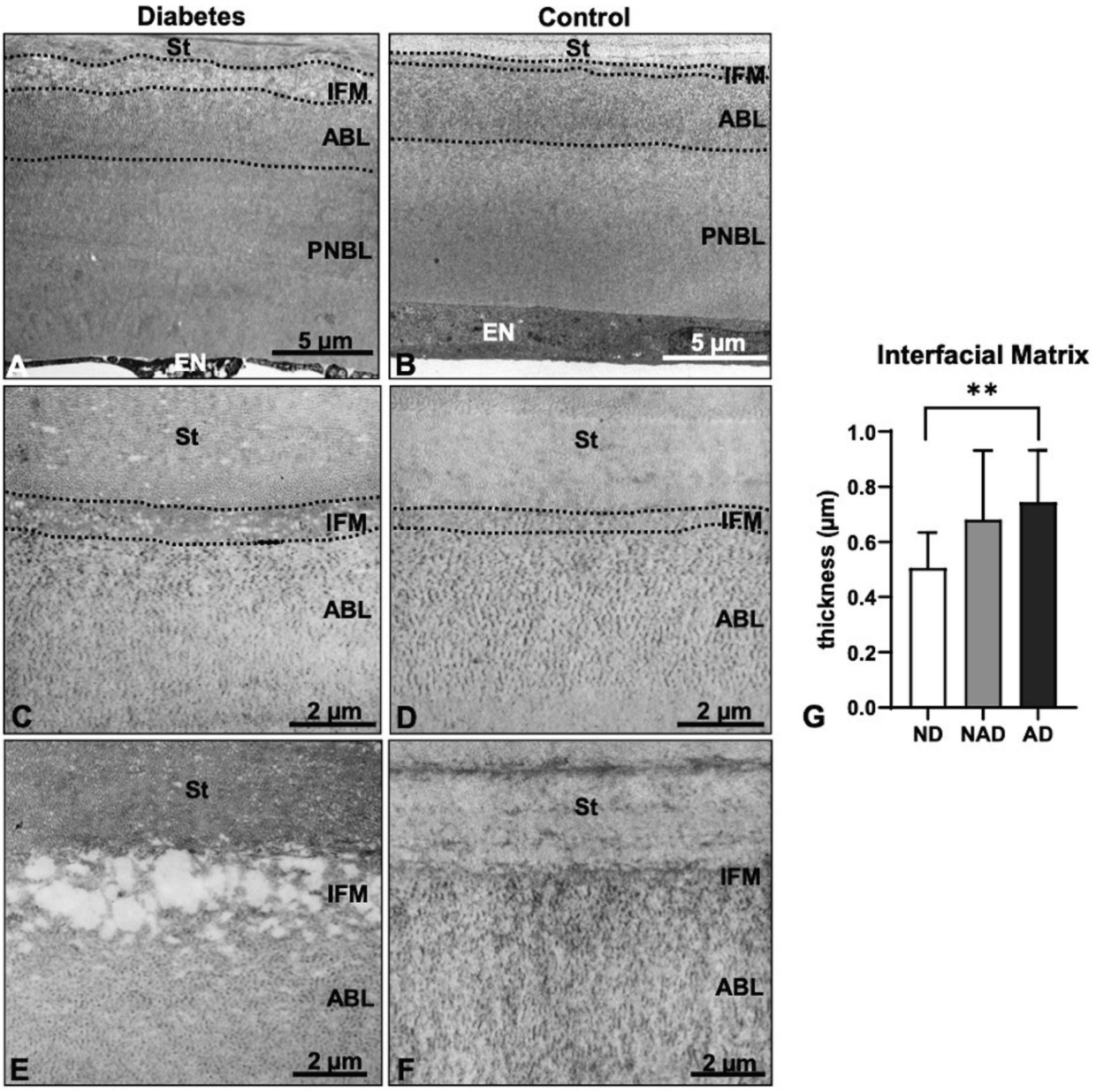

Figure 4. Structural alterations of DM–stroma interface in diabetic corneas differ from the morphology of normal control corneas. (**A**–**F**) Transmission electron micrographs showing thickened IFM (*dotted lines*) with variable amounts of vacuolar inclusions at the DM–stroma interface (**A**, **C**, **E**) in association with diabetes. Alterations are not observed in control corneas. ABL, anterior banded layer of DM; EN, endothelium; PNBL, posterior non-banded layer of DM; St, stroma. (**G**) Quantitative analysis of IFM thickness in ND, NAD, and AD corneas. Data are expressed as means ± SD ($n = 10$ in each group). $^{**}P = 0.003$ (*t*-test).

affecting the posterior corneal endothelium,[18,19] atomic force microscopy was used to quantify tissue integrity and resistance to deformational forces of the DM and endothelium in diabetic and nondiabetic donor corneal tissues prepared for DMEK. We found that the elastic modulus was significantly increased between diabetic and control donor corneal tissue for the DM ($P < 0.0001$) and endothelium ($P < 0.0001$) (Fig. 8). These results indicate abnormally increased stiffness of both the endothelial ECM (DM) face and the apical face of the EDM in diabetic donor corneal tissues prepared for DMEK surgery.

Discussion

Structural changes in the posterior cornea of diabetic donor tissue may explain the known links between diabetes and poorer outcomes after corneal transplantation.[3,8] In vitro cell culture data indicate that hyperglycemia, a main component of uncontrolled diabetes found in the aqueous humor bathing the posterior cornea in vivo, leads to TGFBI protein accumulation and increased AGE formation. That these same changes are found in diabetic donor corneal tissues on transmission electron microscopy and immunohistochem-

Investigative Ophthalmology & Visual Science

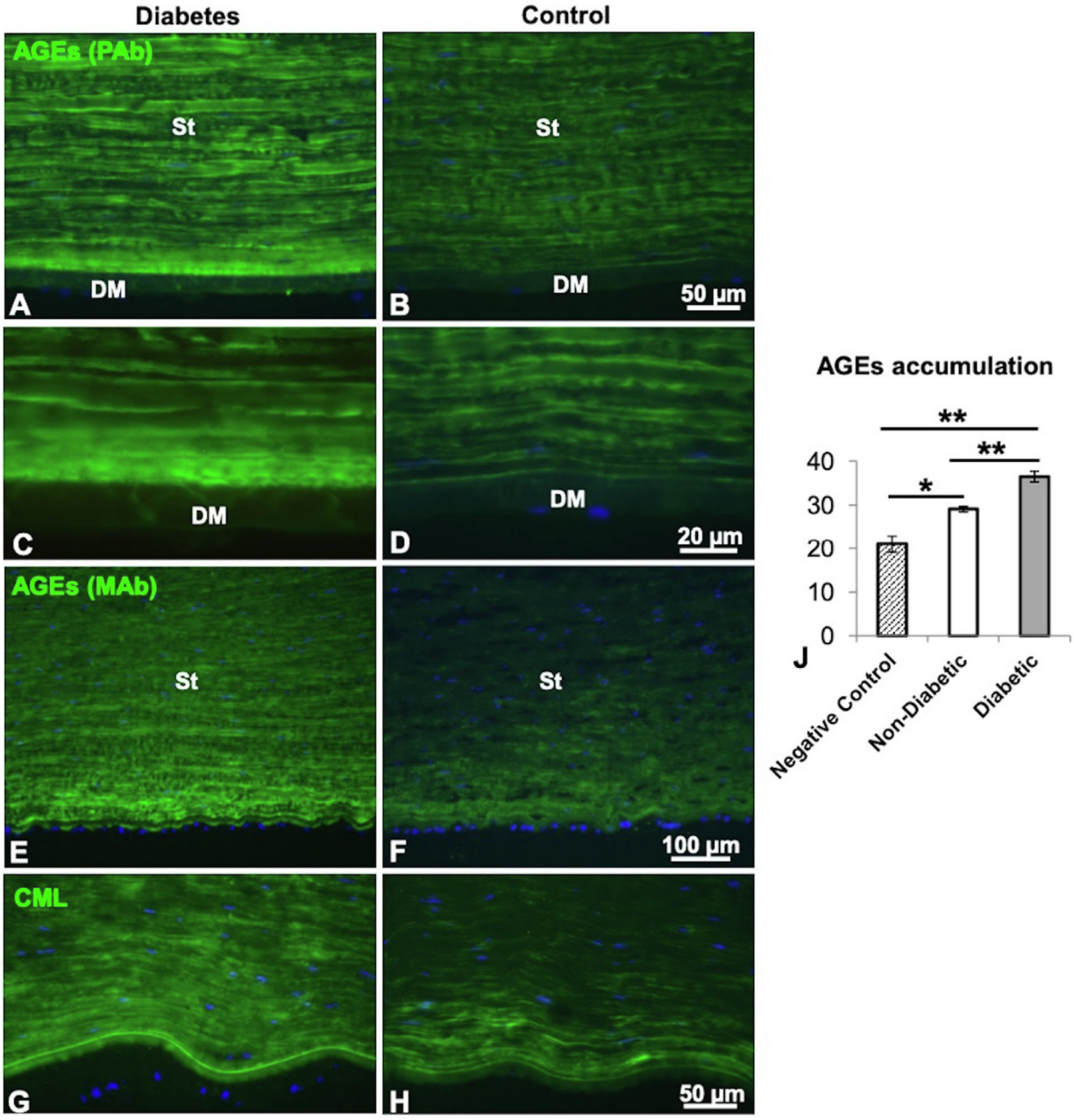

Figure 5. Accumulation of AGEs occurs to a greater extent in diabetic versus normal control corneas. (**A–F**) Immunohistochemical analysis showing differential staining patterns of the posterior corneal stroma (St) and DM–stroma interface region for AGEs using polyclonal (PAb) and monoclonal (MAb) antibodies in diabetic and normal corneas. Nuclei are counterstained with DAPI (*blue*). (**G**, **H**) Immunolocalization of CML, a major epitope of AGEs. (**J**) Quantitative analysis of immunofluorescence signals using ImageJ in negative control sections, nondiabetic control, and diabetic corneas. Data are expressed as means ± SD ($n = 10$ in each group). *$P = 0.004$, **$P < 0.001$ (*t*-test).

istry assays establishes hyperglycemia as a biochemical basis for clinical observations using diabetic donor tissue related to corneal graft preparation and outcomes.[2–5,7–9]

The immunohistochemistry of donor corneal tissues showed markedly increased labeling intensity of adhesive glycoproteins along the DM–stroma interface in diabetic corneas compared to controls, including vitronectin, fibronectin, amyloid P, collagen type IV, and tenascin-C, in addition to TGFBI. TGFBI is present in many tissues, including the eye, where it binds collagen in the ECM and interacts with cell surface integrins facilitating their connection.[20] Skeie and colleagues[5] demonstrated that TGFBI was present in increased amounts in the diabetic EDM versus nondiabetic controls using tandem mass spectrometry. Diabetes has also been associated with changes in ECM proteins in proliferative diabetic retinopathy, including vitronectin, tenascin-C, and amyloid.[21–23] Given that we discovered multiple ECM protein alterations that were conserved between the posterior cornea and the retina of diabetic patients, there may be some basis for clinical alignment of transplant outcomes using diabetic donor tissue and diabetic retinopathy with respect to disease severity.

We demonstrated with light and electron microscopy and double labeling of proteins and AGEs that most adhesive

Investigative Ophthalmology & Visual Science

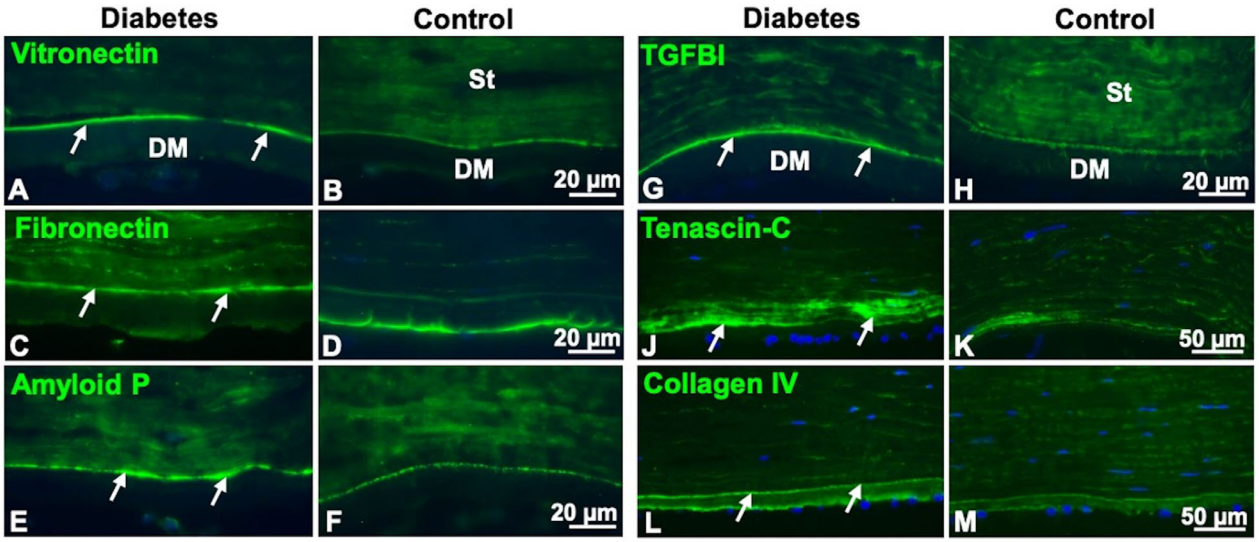

Figure 6. Accumulation of adhesive glycoproteins at the DM–stroma (St) interface in diabetic and normal control corneas. Immunohistochemical analysis shows differential staining patterns of the DM–St interface region (*arrows*) for vitronectin (**A**, **B**), fibronectin (**C**, **D**), amyloid P (**E**, **F**), TGFBI (**G**, **H**), tenascin-C (**J**, **K**), and collagen IV (**L**, **M**). Nuclei are counterstained with DAPI (*blue*). Adhesive glycoprotein labeling intensity was markedly increased in diabetic specimens.

glycoproteins, including vitronectin, fibronectin, amyloid P, and TGFBI, as well as collagen type IV and tenascin-C, were colocalized with AGEs in the IFM of diabetic corneas. Formation of AGE residues on adhesive matrix proteins could explain the increased failure rates of DMEK graft preparation and greater force needed to separate the EDM from stroma in DMEK graft preparation.[7,8] These pathologic alterations are associated with protein aggregation in many chronic diseases. Specifically, the bulky nature of proteins with glycated end products slows proteolysis, which further potentiates the formation of AGEs. Glycated proteins are more resistant to degradation and thus more rapid accumulation. Xu and colleagues[24] demonstrated that the effects of AGEs on the retina are mediated through abnormal structural alterations of the extracellular environment secondary to protein cross-linking, leading to an increase in rigidity of the tissue. Activation of AGE receptors also has been shown to upregulate and induce secretion of pro-inflammatory mediators leading to vascular endothelial dysfunction. Given that blood and aqueous humor glucose concentrations are highly correlated, hyperglycemic aqueous bathing the posterior cornea increases the probability of AGE formation in uncontrolled diabetes.[12,25] Because AGEs and aberrant protein cross-linkages in the retina are clinically pathological, it is likely that similar changes occurring in the posterior cornea are contributing to the poorer clinical outcomes observed with the use of diabetic corneal grafts. AGE accumulation in the posterior cornea, if validated in larger series and clinical trials, may serve as a useful biomarker that correlates with risk for posterior corneal pathology and reduced graft outcomes (e.g., graft preparation failure, reduced postoperative cell density).

Abnormal collagen inclusions were also found in diabetic DMs. Abnormal remodeling of collagen has been demonstrated in the DMs of corneas with endothelial dystrophies and shown to lose its typical hexagonal lattice configuration.[26] AGEs, specifically on collagen, have been shown to increase the stiffness of the ECM, leading to organ and vessel dysfunction throughout the body.[27] Increased tissue rigidity may be related to the greater force needed to separate tissues in graft preparation for DMEK corneal transplants that our group characterized previously.[9] The EDM separates from the underlying stroma at the IFM in DMEK graft preparation.[28] It is unclear whether the majority of the IFM is left behind with stroma or pulled with the DMEK graft during failed DMEK graft preparation in diabetic tissues; either scenario may occur, as documented previously in DMEK graft preparation failures using donor corneas that were not characterized with respect to diabetes status.[29,30]

Finally, in order to investigate the biomechanical impact of diabetes on the health of the EDM, we used AFM to measure tissue resistance to deformational forces in diabetic and nondiabetic donor corneas. We observed that diabetic corneas have a stiffer ECM (higher elastic modulus) at the DM face, which holds potential clinical relevance to the function of all donor and patient corneas given the importance of ECM composition and stiffness to CEC function.[18,19] Specifically, ECM stiffness has been shown to have a pathological impact on CEC health in other diseases affecting the corneal endothelium. In Fuchs endothelial corneal dystrophy (FECD), biomechanical data obtained by performing AFM on the DMs of FECD patient samples obtained from surgery, as well as FECD mice with a *COL8A2* mutation that models early-onset disease, demonstrate that DMs in FECD have a lower elastic modulus and are softer than those of unaffected controls.[18,19] Importantly, the changes observed in matrix softness in the *COL8A2* FECD mouse model preceded CEC loss, indicating a negative functional impact to cell health secondary to matrix substrate stiffness. In both cases of higher (diabetes) or lower (FECD) ECM stiffness, alterations in ECM resistance to deformation compared to healthy tissues may be associated with pathology in characteristic CEC functions such as ion/fluid pumping and barrier integrity, as well as cell viability. Further investigations into the temporal sequence of pathological events in diabetes could further illuminate the interplay between ECM changes and intracellular functions. Addition-

Investigative Ophthalmology & Visual Science

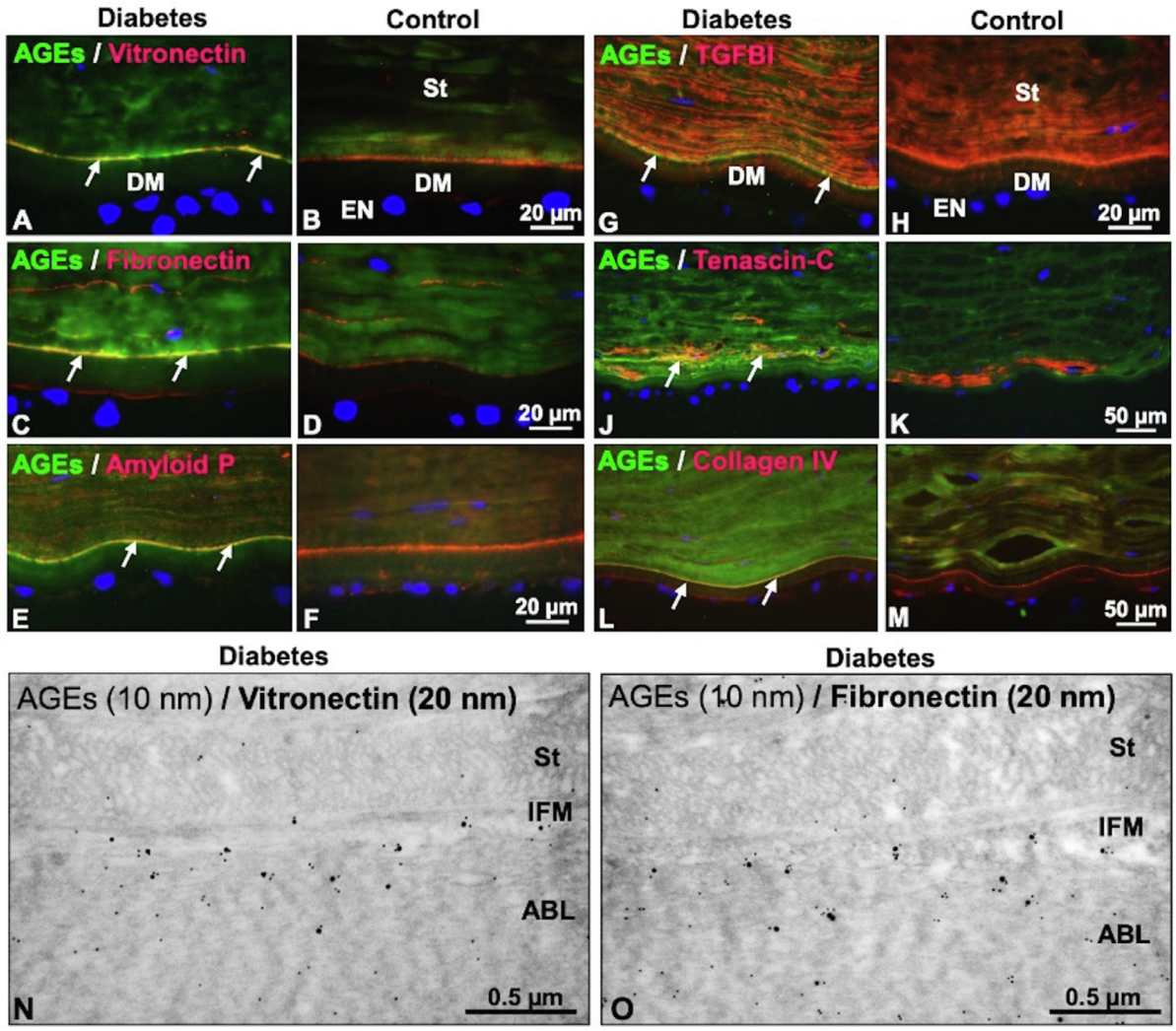

Figure 7. Colocalization of adhesive glycoproteins with AGEs at the DM–stroma (St) interface in diabetic and normal control corneas. (**A**–**M**) Immunohistochemical double-labeling experiments showing differential staining patterns of the DM–St interface region (*arrows*) for AGEs and vitronectin (**A**, **B**), fibronectin (**C**, **D**), amyloid P (**E**, **F**), TGFBI (**G**, **H**), tenascin-C (**J**, **K**), and collagen IV (**L**, **M**). Nuclei are counterstained with DAPI (*blue*). EN, endothelium. (**N**, **O**) Immunogold double-labeling for AGEs (10-nm gold particles) and vitronectin (**N**) or fibronectin (**O**) (20-nm gold particles) in the IFM of diabetic corneas. ABL, anterior banded layer of the DM. These results indicate that AGE residues are localized specifically to the adhesive matrix proteins in the interfacial matrix of diabetic tissues.

ally, AFM data from our experiment indicated the presence of a mechanically stiffer apical face in diabetic tissues. Interestingly, this finding corresponds to the CEC blebbing and abnormally darkened aqueous-facing membrane that we demonstrated in previously work performing transmission electron microscopy on DMEK graft tissues.[4] Clinical implications for the changes observed at the apical face of the corneal endothelium require additional investigation.

Limitations of this study relate to the categorization of donor tissues by diabetes status and sample sizes of donor tissues. A historical and retrospective methodology was utilized to collect donor medical histories from the review of eye banking and medical records at the time of donor death. As such, we were unable to incorporate more objective factors of diabetic disease such as duration and hemoglobin A1c levels, and we did not account for the impact of associated comorbidities such as hypertension and obesity. Nonetheless, we utilized the same disease category definitions as several other published investigations in this area,[2,4,5] and our data will help provide an important evidentiary basis and basic scientific context for forthcoming prospective clinical trial data generated from the Diabetes Endothelial Keratoplasty Study (ClinicalTrials.gov identifier NCT05134480). Regarding quantitative AGE analysis in our cell culture model, we did not perform a statistical analysis for significant differences due to the intention to compare groups on a qualitative basis using this model. Regarding donor cornea assays, we were unable to compare endothelial cell densities due to the limited number of corneas studied and wide variation among tissues. Additionally, we were unable to perform immunohistochemistry or AFM testing on tissues that underwent tears during graft preparation due to sample destruction.

Taken altogether, our findings provide further evidence that diabetes and hyperglycemia alter CEC ECM structure and biochemical composition, including alterations in the DM that lead to thickening and stiffening. Our analysis indicates that abnormal ECM composition and physical

Investigative Ophthalmology & Visual Science

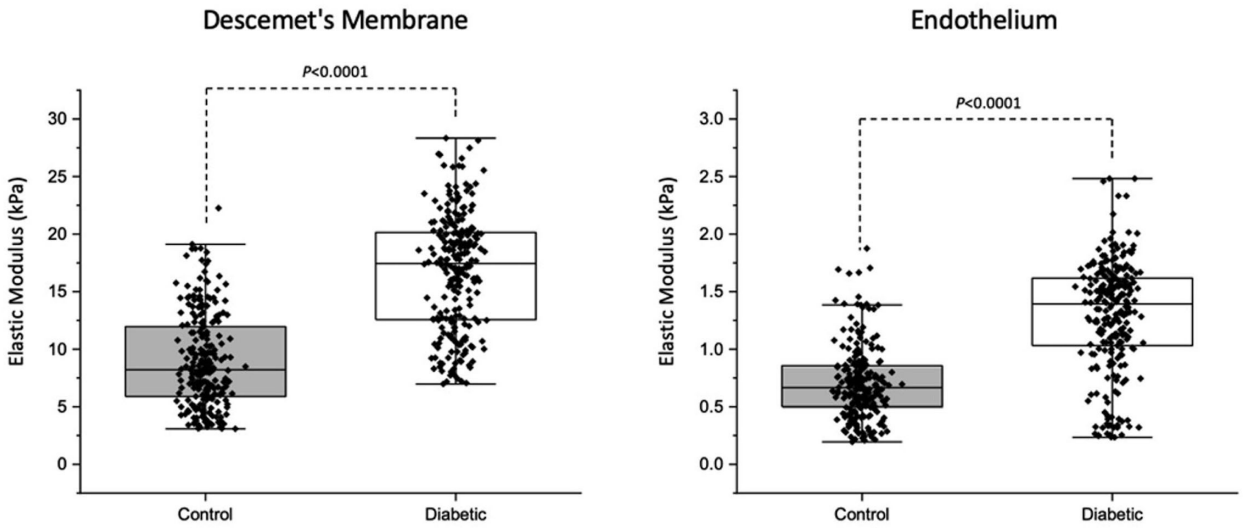

Figure 8. The DM and endothelium were markedly stiffer in diabetic versus control corneas as determined by atomic force microscopy. The elastic modulus was measured in six diabetic and six age-matched control corneas and was significantly greater at 16.77 ± 5.01 and 8.95 ± 4.07 kPa for the DM and 1.29 ± 0.48 and 0.70 ± 0.31 kPa for the endothelium, respectively ($P < 0.0001$). Box plots depict the median (*solid line*) and 25th and 75th percentiles, and whiskers show the 10th and 90th percentiles. *Black circles* indicate individual measurements.

properties observed in diabetic donor corneal tissue, including the pathological accumulation of ECM proteins modified by nonenzymatic glycation at the DM–stroma interface, are likely to contribute to failures in corneal graft preparation that have been well documented with the use of diabetic donor tissues, and they may be related to cell functional abnormalities documented in prior studies. However, it remains unclear whether this increase in tissue stiffness is attributable to increased tissue thickness, altered protein expression, or both. The results in this series lay the foundation for clinically relevant future investigations into the impact of diabetes on DMEK graft scrolling behavior and the reversibility of diabetic posterior corneal alterations with improvements in glycemic control. The results of our study may also lead to the development of AGE accumulation in the EDM as a useful biomarker for determining the impact of diabetes on posterior corneal tissue.

Acknowledgments

Supported in part by the M.D. Wagoner & M.A. Greiner Cornea Excellence Fund, the Beulah and Florence Usher Chair in Cornea/External Disease and Refractive Surgery, the University of Iowa Hospitals & Clinics Cornea Research Fund, Mr. and Mrs. Robert and Joell Brightfelt, Mr. and Mrs. Lloyd and Betty Schermer, a grant from the National Institutes of Health (R01EY016134 to SMT), and an Eye Bank Association of America Pilot Research Grant.

Disclosure: **K.D. Kingsbury**, None; **J.M. Skeie**, None; **K. Cosert**, None; **G.A. Schmidt**, None; **B.T. Aldrich**, None; **C.S. Sales**, None; **J. Weller**, None; **F. Kruse**, None; **S.M. Thomasy**, None; **U. Schlötzer-Schrehardt**, None; **M.A. Greiner**, None

References

1. Centers for Disease Control and Prevention. National diabetes statistics report. Available from: https://www.cdc.gov/diabetes/data/statistics-report/index.html. Accessed June 8, 2023.
2. Liaboe CA, Aldrich BT, Carter PC, et al. Assessing the impact of diabetes mellitus on donor corneal endothelial cell density. *Cornea*. 2017;36(5):561–566.
3. Lass JH, Benetz BA, Patel SV, et al. Donor, recipient, and operative factors associated with increased endothelial cell loss in the cornea preservation time study. *JAMA Ophthalmol*. 2019;137(2):185–193.
4. Aldrich BT, Schlötzer-Schrehardt U, Skeie JM, et al. Mitochondrial and morphologic alterations in native human corneal endothelial cells associated with diabetes mellitus. *Invest Ophthalmol Vis Sci*. 2017;58(4):2130–2138.
5. Skeie JM, Aldrich BT, Goldstein AS, Schmidt GA, Reed CR, Greiner MA. Proteomic analysis of corneal endothelial cell-descemet membrane tissues reveals influence of insulin dependence and disease severity in type 2 diabetes mellitus. *PLoS One*. 2018;13(3):e0192287.
6. Ali M, Raghunathan VK, Li JY, Murphy CJ, Thomasy SM. Biomechanical relationships between the corneal endothelium and Descemet's membrane. *Exp Eye Res*. 2016;152:57–70.
7. Greiner MA, Rixen JJ, Wagoner MD, et al. Diabetes mellitus increases risk of unsuccessful graft preparation in Descemet membrane endothelial keratoplasty: a multicenter study. *Cornea*. 2014;33(11):1129–1133.
8. Vianna LM, Stoeger CG, Galloway JD, et al. Risk factors for eye bank preparation failure of Descemet membrane endothelial keratoplasty tissue. *Am J Ophthalmol*. 2015;159(5):829–834.e2.
9. Schwarz C, Aldrich BT, Burckart KA, et al. Descemet membrane adhesion strength is greater in diabetics with advanced disease compared to healthy donor corneas. *Exp Eye Res*. 2016;153:152–158.
10. Levy SG, McCartney AC, Moss J. The distribution of fibronectin and P component in Descemet's membrane: an immunoelectron microscopic study. *Curr Eye Res*. 1995;14(9):865–870.
11. Naguib YW, Saha S, Skeie JM, et al. Solubilized ubiquinol for preserving corneal function. *Biomaterials*. 2021;275:120842.
12. Gomel N, Barequet IS, Lipsky L, Bourfa N, Einan-Lifshitz A. The effect of the glycemic control on the aqueous

humor glucose levels in diabetic patients undergoing elective cataract surgery. *Eur J Ophthalmol*. 2021;31(2):415–421.

13. Schlötzer-Schrehardt U, Bachmann BO, Tourtas T, et al. Ultrastructure of the posterior corneal stroma. *Ophthalmology*. 2015;122(4):693–699.
14. Zadravec P, Braunger BM, Melzer B, et al. Transgenic lysyl oxidase homolog 1 overexpression in the mouse eye results in the formation and release of protein aggregates. *Exp Eye Res*. 2019;179:115–124.
15. Morgan JT, Raghunathan VK, Thomasy SM, Murphy CJ, Russell P. Robust and artifact-free mounting of tissue samples for atomic force microscopy. *Biotechniques*. 2014;56(1):40–42.
16. Chang YR, Raghunathan VK, Garland SP, Morgan JT, Russell P, Murphy CJ. Automated AFM force curve analysis for determining elastic modulus of biomaterials and biological samples. *J Mech Behav Biomed Mater*. 2014;37:209–218.
17. Reddy S, Bichler J, Wells-Knecht KJ, Thorpe SR, Baynes JW. N epsilon-(carboxymethyl)lysine is a dominant advanced glycation end product (AGE) antigen in tissue proteins. *Biochemistry*. 1995;34(34):10872–10878.
18. Xia D, Zhang S, Nielsen E, et al. The ultrastructures and mechanical properties of the Descemet's membrane in Fuchs endothelial corneal dystrophy. *Sci Rep*. 2016;6:23096.
19. Leonard BC, Jalilian I, Raghunathan VK, et al. Biomechanical changes to Descemet's membrane precede endothelial cell loss in an early-onset murine model of Fuchs endothelial corneal dystrophy. *Exp Eye Res*. 2019;180:18–22.
20. Han B, Luo H, Raelson J, et al. TGFBI (βIG-H3) is a diabetes-risk gene based on mouse and human genetic studies. *Hum Mol Genet*. 2014;23(17):4597–4611.
21. Esser P, Bresgen M, Weller M, Heimann K, Widermann P. The significance of vitronectin in proliferative diabetic retinopathy. *Graefes Arch Clin Exp Ophthalmol*. 1994;232(8):477–481.
22. Mitamura Y, Takeuchi S, Ohtsuka K, Matsuda A, Hiraiwa N, Kusakabe M. Tenascin-C levels in the vitreous of patients with proliferative diabetic retinopathy. *Diabetes Care*. 2002;25(10):1899.
23. Gillmore JD, Hawkins PN, Pepys MB. Amyloidosis: a review of recent diagnostic and therapeutic developments. *Br J Haematol*. 1997;99(2):245–256.
24. Xu J, Chen L-J, Yu J, et al. Involvement of advanced glycation end products in the pathogenesis of diabetic retinopathy. *Cell Physiol Biochem*. 2018;48(2):705–717.
25. Fortenbach CR, Skeie JM, Sevcik KM, et al. Metabolic and proteomic indications of diabetes progression in human aqueous humor. *PLoS One*. 2023;18(1):e0280491.
26. Walckling M, Waterstradt R, Baltrusch S. Collagen remodeling plays a pivotal role in endothelial corneal dystrophies. *Invest Ophthalmol Vis Sci*. 2020;61(14):1.
27. Ott C, Jacobs K, Haucke E, Santos AN, Grune T, Simm A. Role of advanced glycation end products in cellular signaling. *Redox Biol*. 2014;2:411–429.
28. Schlötzer-Schrehardt U, Bachmann BO, Laaser K, Cursiefen C, Kruse FE. Characterization of the cleavage plane in Descemet's membrane endothelial keratoplasty. *Ophthalmology*. 2011;118(10):1950–1957.
29. Kruse FE, Lasser K, Cursiefen C, et al. A stepwise approach to donor preparation and insertion increases safety and outcome of Descemet membrane endothelial keratoplasty. *Cornea*. 2011;30(5):580–587.
30. Schlötzer-Schrehardt U, Bachmann BO, Tourtas T, et al. Reproducibility of graft preparations in Descemet's membrane endothelial keratoplasty. *Ophthalmology*. 2013;120(9):1769–1777.